Development of the Handheld Measuring Probe for a 3D Scanner

Robert Kupiec [ID], Wiktor Harmatys [ID], Izabela Sanetra [ID], Katarzyna Składanowska [ID], and Ksenia Ostrowska[(✉)] [ID]

Laboratory of Coordinate Metrology, Cracow University of Technology, al. Jana Pawła II 37, 31-864 Cracow, Poland
ksenia.ostrowska@pk.edu.pl

Abstract. This paper presents a specially designed contact measuring probe for the 3D scanner. It also presents stages of development of the handheld measuring probe including adjustment on coordinate measuring machine. The test procedure of the system was performed according to VDI/VDE 2634. This procedure involved the determination of probing error, sphere spacing error and flatness measurement error. The performance of the system was verified according to the test procedure. The maximum permissible errors of the system were determined and the measurement uncertainty was taking into account. The accuracy of the system has been improved thanks to the use of the probe calibration on the coordinate measure machine.

Keywords: 3D scanner · Validation · Handheld probes · Markers

1 Introduction

The popularity of three-dimensional 3D scanning technologies have increased over the last few years. This is a result of technological progress for example, scanners are smaller, more portable and more powerful. Furthermore, we can observe increasing range of different applications in multiple industries [1, 2].

The test results described in this article are based on measurements taken by the scanner, such as MICRON3D green stereo (Fig. 1). Depending on the technology we use, there are scanner based the projection of structured light and laser projection. In this research we use structured light scanner with two cameras and one projector. In this scanner, the principle of operation is based on passive triangulation between each camera, projector and measuring point. Geometry mapping is carried out by projecting structured light onto the scanned surface according to the Grey code principle and phase shifted fringes. The MICRON 3D green stereo scanner uses to measure green LED light, with a wavelength of around 500 nm, which enables increase the accuracy of the measurement; even 30% in relation to the traditional method of white light measurement. The use of monochrome cameras enable to create better mapping of the surface structure. In addition, the usage of LED light source reduces energy consumption and increases the service life of the entire system.

All results are based on measurements using the contact probe with determined markers and the 3D scanner. The markers placed on the probe are necessary to determine the position of the probe in the measuring space of the optical scanner - the markers are tracked by the scanner. The handheld probe is used to measure elements most often invisible to the scanner for example internal holes. This contact probe is useful for measuring process in which the scanner may have an obstacle to measure complicated objects [3–9].
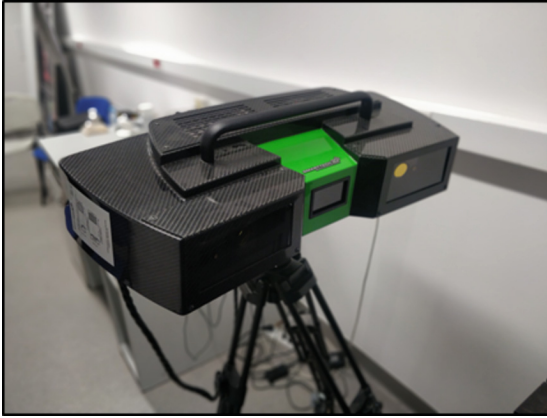
Fig. 1. Scanner MICRON 3D green stereo.

2   Stages of Development of the Tactile Probe

Development of contact probe had several important stages. The first step was the choice of appropriate markers. This part of research was aimed at selecting a material that would ensure the most appropriate representation of the marker in the image made by the scanner detector. Research work was carried out for cameras operating in the visible and infrared beams. The selection of markers was influenced by the shape of the probe and the number of points needed for a reliable identification on the probe in the measurement space. The possibility of their calibration on a more accurate device than the designed system was also taken into account.

At the beginning, tests were carried out with passive markers (Fig. 2), which were in the form of stickers or a printout on the probe. After testing, it turned out that the passive markers were insufficient, the main problem was the inability to precisely calibrate them.

Fig. 2. Probe with passive markers.

Therefore, it was decided to choose active markers - diodes placed in conical holes on the surface of the probe (Fig. 3).

Fig. 3. Probe with active markers.

The next aspect considered was the shape of the probe. Various variants of the measuring probe were developed: due to their design and the arrangement of markers on the probe. Work was carried out on ergonomics, functionality and the appearance of the probe.

The next stage was to calibrate the probe. In the probe with active markers, the measurement of markers was performed with the Leitz PMM 12106 with increased $MPE = 0.6\ \mu m + 0.7\ L\ \mu m/m$ with a contact probe head. After mounting the matting plate, a stand for measurements was made so that the plate would not bend. Then, the markers were measured from both sides of the probe to determine the centers of the markers (Fig. 4). These coordinates were created at the intersection of the axis of the inner cone with the matting plate.

Each measurement was performed using an accredited method of calibrating objects, the so-called multi-position method. This method consists of measuring an element in four positions: base, object rotated about the x axis, object rotated about the y axis, object rotated about the z axis. Probes with active markers were calibrated with an uncertainty of 1.1 μm.
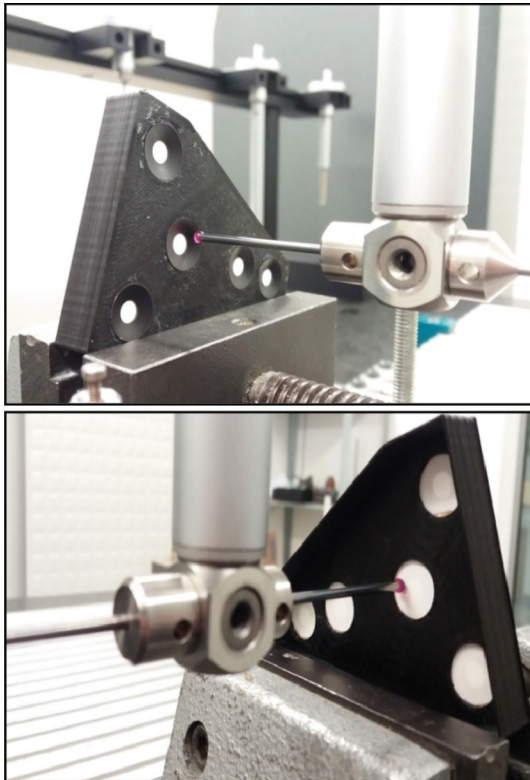
Fig. 4. Probe with active markers measured by WMP PMM.

An important element in the development of the probe is to define the algorithm of the x, y, z coordinates of the probe tip center. It must be calculated in relation to the centers of the markers obtained from CMM (Coordinate Measuring Machine) measurements. Measurements carried out on coordinate measuring machine was a key to improvement the accuracy of the measuring probe [10, 11]. For further research, it was necessary to develop a computer program allowing to determine the probe tip center based on the markers.

3 Validation of the Alignment of Coordinate System

In order to increase the accuracy of the measuring probe, a number of tests were carried out to check the algorithms used by the probe. The alignment of the coordinate system has been validated. The validation consisted in converting 4 points measured in the coordinate system (local system B) using the contact probe to the coordinate system of the scanner (global system A). The standard shown in Fig. 5 was used during the research. This standard consists of 3 balls and 3 cones.
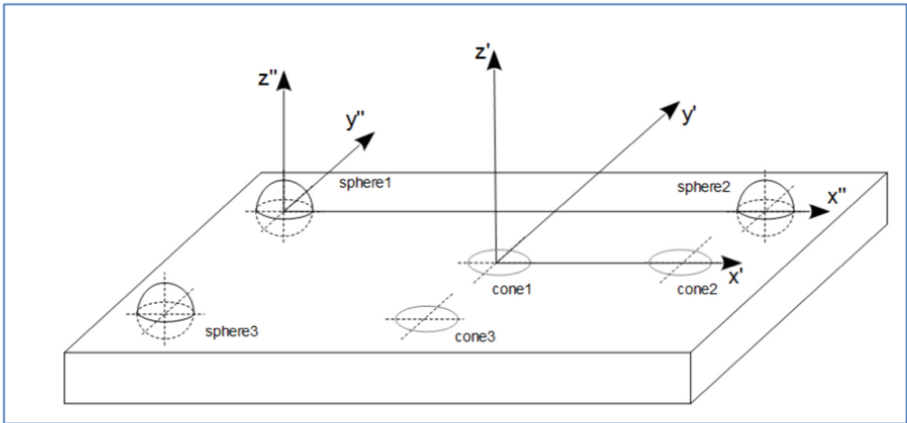
Fig. 5. Validation standard.

Two possible methods of solving the problem were validated:

– method 1 - in this method, using a contact probe, the centers of three spheres (Fig. 5.) and the points to be converted to the coordinate system of the scanner are measured. On the other hand, in the coordinate system of the scanner, the centers of three spheres should be determined, which enables the conversion of points from the contact system to the contactless system.
– method 2 - in this method, three cones (one point in each of the three cones) and the points to be converted to the coordinate system of the scanner are measured using the contact probe. On the other hand, in the coordinate system of the scanner, the centers of three spheres should be determined, which enables the conversion of points from the contact system to the contactless system.

4 Validation of the Developed Program

VALIDATION METHOD 1.
Four points were measured using a contact probe (local system B) (Table 1):

Table 1. Input data.

	x [mm]	y [mm]	z [mm]
1	−114.08241	145.11110	481.95486
2	16.65738	135.72185	828.41166
3	216.00668	140.53416	719.08103
4	−3.15570	147.95254	417.38023

These points were entered into the reference software (PC-DMIS). They were then transformed according to method 1. The Table 2 shows the coordinates of the four points after conversion in the reference software (PC-DMIS). These results were taken as reference results (PC-DMIS software is certified metrology software).

Table 2. Reference results.

	x [mm]	y [mm]	z [mm]
1	110.58510	−118.43115	100.41587
2	189.05822	91.48571	−194.52522
3	395.10355	93.15632	−98.30144
4	225.75765	−119.41121	157.13459

The next step was to recalculate the input data (Table 1) in the validated software. The converted coordinates of the points obtained from the validated software are presented in Table 3. The differences between these results and the reference results are listed in the Table 4.

Table 3. Results from validated software.

	x [mm]	y [mm]	z [mm]
1	110.58509	−118.43115	100.41587
2	189.05823	91.48572	−194.52522
3	395.10356	93.15631	−98.30144
4	225.75765	−119.41122	157.13459

Table 4. Differences between the results of the validated program and the reference results (method 1).

	x [mm]	y [mm]	z [mm]
1	−0.00001	0.00000	0.00000
2	0.00001	0.00001	0.00000
3	0.00001	−0.00001	0.00000
4	0.00000	−0.00001	0.00000

The largest differences observed were $\pm 0.01\ \mu m$. Software errors can be considered as irrelevant.

VALIDATION METHOD 2.

The same input data presented in Table 1 was used to validate method 2. And the same reference data (Table 2). The next step was to recalculate the input data in the validated software. The converted coordinates of the points obtained from the validated software are presented in Table 5. Table 6 shows the differences between the results from Tables 2 and 5.

Table 5. Results from validated software.

	x [mm]	y [mm]	z [mm]
1	110.04645	−118.47225	100.11343
2	190.78408	91.61205	−194.09633
3	396.07815	93.24531	−96.27933
4	224.77652	−119.47480	157.72157

Table 6. Differences between the results of the validated program and the reference results (method 2).

	x [mm]	y [mm]	z [mm]
1	−0.53865	−0.04110	−0.30244
2	1.72586	0.12634	0.42889
3	0.97460	0.08899	2.02211
4	−0.98113	−0.06359	0.58698

The biggest difference that was observed between the results obtained from the validated program and the reference results in method 2 was 2.022 mm. The errors of the second method are much bigger than that of the first method.

5   System Calibration Procedure

To check the accuracy of the measurement, an accredited calibration procedure of the optical system was used, based on VDI/VDE 2634. This section presents the accuracy of the contact head. According to VDI/VDE, parameters are measured: probing error (form) PF, probing error (size) PS, sphere spacing error SD and flatness measurement error F [12, 13].

The probing error describes a characteristic error in 3D optical measuring systems based on surface scanning in a small measuring range. It is the distance between the center of the sphere determined using the Gaussian criterion (the method of least squares) [14].

As a standard, spheres made of ceramics, steel or other materials adequately diffusing light with a diameter of:

$$d = (0, 1 \ldots 0, 02) \bullet L_0 \tag{1}$$

where:

L_0 - diagonal of the smallest rectangular parallelepiped encompassing the measurement space. The procedure consists in measuring the ball in at least 10 settings throughout the measurement space (Fig. 6).
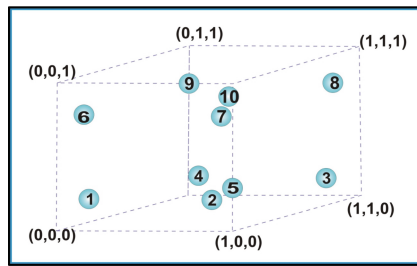
Fig. 6. Distribution of the test ball throughout the measurement space of the system during the measurement.

Another qualitative parameter, the sphere spacing error, is used to verify the ability of the system to reconstruct the length. It is the difference between the measured value and the calibrated distance between the balls:

$$\Delta l = lm - lk \tag{2}$$

where:

Δl - error of the distance between the centers of the spheres,

lm - measured length value,

lk - calibrated length value.

To test the error of the distance between the centers of the spheres, a ball-bar standard witch two spheres made of steel, ceramics or other appropriate materials can be used. In order to investigate the error of indication along the length, the standard is measured in six settings (Fig. 7).
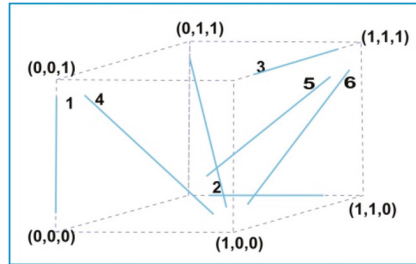
Fig. 7. The arrangement for determination of the sphere spacing error.

Flatness measurement error is defined as the range of distances of the points measured from the plane constructed according to the least squares method by the best fit. Standards in the form of cuboids made of steel, ceramics, aluminum or other material with low reflectivity are used here, the width of which cannot be less than 50 mm, and length than $0,5 \bullet L_0$. In order to determine the flatness measurement error, a measurement should be made in min. six settings (Fig. 8).
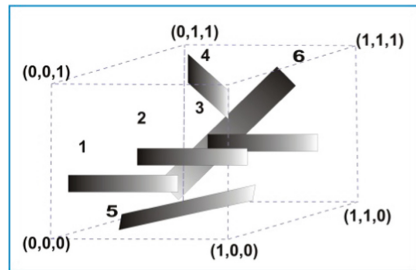
Fig. 8. The arrangement for determination of the flatness measurement error.

6   Results of Calibration

A reference ball was used to determine the error of the probing error (form) PF and the probing error (size) PS. During the measurement, this sphere was positioned so as to cover the entire measuring space. Each time, 25 points were collected evenly distributed on the sphere. As can be seen from the values presented in Table 1, MPE (PF) is 0.031 mm, while MPE (PS) is 0.026 mm. MPE values take into account the measurement uncertainty of the standard during its calibration (Table 7).

Table 7. The results of the determination of the probing error. Nominal value of the reference ball diameter is 24.98093 mm.

Position	PF	U(PF)	Measured diameter	PS	U(PS)
	[mm]	[mm]	[mm]	[mm]	[mm]
1	0.0241	0.0014	24.9717	0.0092	0.0006
2	0.0173	0.0014	24.9778	0.0031	0.0006
3	0.0183	0.0014	24.9608	0.0201	0.0006
4	0.0292	0.0014	24.9612	0.0197	0.0006
5	0.0021	0.0014	24.9590	0.0219	0.0006
6	0.0119	0.0014	24.9554	0.0255	0.0006
7	0.0277	0.0014	24.9622	0.0187	0.0006
8	0.0176	0.0014	24.9608	0.0201	0.0006
9	0.0211	0.0014	24.9747	0.0062	0.0006
10	0.0282	0.0014	24.9717	0.0092	0.0006

Max(PF) 0.0292 mm Max(PS) 0.0255 mm.
MPE(PF) 0.0310 mm MPE(PS) 0.0260 mm.

Another parameter checked was the sphere spacing error SD. Setting the standard during the measurement was consistent with Fig. 6. For each of the 7 measurements, the parameter was calculated as the absolute value of the difference between the measured value Lz and the nominal value Ln, $SD = |Lz - Ln|$. The MPE (SD) value was determined at the level of 0.0290 mm (Table 8).

Table 8. Measurement results of the length standard.

Position	L_z	L_n	SD	U
	[mm]	[mm]	[mm]	[mm]
X	269.3813	269.4036	0.0223	0.0007
Y	269.3893	269.4036	0.0143	0.0007
Z1	269.3955	269.4036	0.0081	0.0007
D1	269.4247	269.4036	−0.0211	0.0007
D2	269.4234	269.4036	−0.0198	0.0007
D3	269.4254	269.4036	−0.0218	0.0007
D4	269.4315	269.4036	−0.0279	0.0007

Max(SD) 0.0279 mm.
MPE(SD) 0.0290 mm.

The last of the determined parameters was the flatness error, where the standard was set in the measurement space as shown in Fig. 7. The maximum flatness error was determined at the level of MPE (F) = 0.034 mm (Table 9).

Table 9. Flatness error results.

Position	F	U
	[mm]	[mm]
1	0.0138	0.0026
2	0.0232	0.0026
3	0.0312	0.0026
4	0.0282	0.0026
5	0.0186	0.0026
6	0.0277	0.0026

Max(F) 0.0312 mm.
MPE(F) 0.0340 mm.

All the parameters of the tested system have been determined according to VDI/VDE 2634. The parameters such as maximum permissible errors (MPE) was determined.

7 Conclusions

Optical measurements are very important in industry today. They are very profitable from an economic point of view. We can measure many features at once in a short period of time. However, 3D scanners are not able to measure all dimensions. Sometimes the measurements require collecting points in places not visible by the 3D scanner. The contact measuring probe is more suitable for such applications.

Many problems have been solved during the research. Passive markers are easier to apply than active markers. On the other hand, active markers allow you to achieve more accurate results.

The correct determination of the marker centers allowed to improve the accuracy of the measuring probe. This was made possible by measuring the marker centers on coordinate measuring machine.

The measuring system consisting of the 3D scanner and the handheld measuring probe was successfully tested according to VDI/VDE 2634 [14]. The system parameters were determined in accordance with metrological requirements and the measurement uncertainty was taking into account.

The software module responsible for the alignment of coordinate systems was validated. The software enables alignment by two methods. The validation of method one showed that the software had negligibly small errors. The validation of the second method showed that the errors are much larger than for the first method, so it is recommended to use method 1 as it gives less errors. The biggest limitation of using handheld probe is

the reduced measuring space in relation to the space of the entire system. If the markers on the probe (even one) are invisible to the system, the algorithm is unable to calculate where the measuring tip is located.

Further work will involve the preparation of a correction matrix for the described probe, using reference measuring machines.

References

1. Owczarek, D., Ostrowska, K., Sładek, J.: Examination of optical coordinate measurement systems in the conditions of their operation. J. Mach. Constr. Maintenance Probl. Eksploatacji **4**, 7–19 (2017)
2. Owczarek, D., Ostrowska, K., Harmatys, K., Sładek, J.: Estimation of measurement uncertainty with the use of uncertainty database calculated for optical coordinate measurements of basic geometry elements. Adv. Sci. Technol. Res. J. **9**(27), 112–117 (2015). https://doi.org/10.12913/22998624/59092
3. Juras, B., Szewczyk, D.: Dokładność pomiarów realizowanych skanerem optycznym, Postępy Nauki i Techniki, Politechnika Lubelska 7 (2011)
4. Urbas, U., Zorko, D., Černe, B., Tavčar, J., Vukašinović, N.: A method for enhanced polymer spur gear inspection based on 3D optical metrology. Measurement **169** (2021)
5. Helle, R.H., Lemu, H.G.: A case study on use of 3D scanning for reverse engineering and quality control. Mater. Today Proc. **45**(Part 6), 5255–5262 (2021)
6. Sładek, J.: Dokładność pomiarów współrzędnościowych, Wydawnictwo Politechniki Krakowskiej, Kraków (2011)
7. Sitnik, R.: Odwzorowanie kształtu obiektów trójwymiarowych z wykorzystaniem oświetlenia strukturalnego, Oficyna Wydawnicza Politechniki Warszawskiej (2010)
8. Sitnik, R.: New method of structure light measurement system calibration based on adaptive and effective evaluation of 3D-phase distribution. Proc. SPIE, Opt. Meas. Syst. Ind. Inspection IV, **5856**, 109–117 (2005)
9. Song, M., Chen, F., Brown, G.M.: Overview of 3-D shape measurement using optical methods. Opt. Eng. **39**, 10–22 (2000)
10. Kupiec, M.: Optyczno-stykowa metoda pomiarów współrzędnościowych, Ph.D. thesis, Politechnika Krakowska (2007)
11. Bernal, C., de Agustina, B., Marín, M.M., Camacho, A.M.: Performance evaluation of optical scanner based on blue LED structured light. Procedia Eng. **63**, 591–598. The Manufacturing Engineering Society International Conference, MESIC (2013)
12. Bonin, R., Khameneifar, F., Mayer, J.R.R.: Evaluation of the metrological performance of a handheld 3D laser scanner using a pseudo-3D ball-lattice artifact. Sensors (2021)
13. Ostrowska, K., Szewczyk, D., Sładek, J.: Optical systems calibration according to ISO standards and requirements of VDI/VDE. Wzorcowanie systemów optycznych zgodnie z normami ISO i zaleceniami VDI/VDE. Technical Transactions. Mechanics (2012)
14. VDI-VDE-2634-Systeme mit flaechenhafter Antastung (2013)